Received: 9 March 2018 | Revised: 25 August 2018 | Accepted: 26 August 2018

DOI: 10.1002/jrs.5485

RESEARCH ARTICLE

WILEY Journal of RAMAN SPECTROSCOPY

Joint sparse representation and denoising method for Raman spectrum

Zheng Fang[1,3] | Yu Tao[2] | Wen Wang[1,3] | Wenxin Zhang[1] | Lingfeng Duan[4] | Ying Liu[1,3] | Changchun Yan[1,3] | Lulu Qu[5] | Caiqin Han[1,3]

[1]Jiangsu Key Laboratory of Advanced Laser Materials and Devices, School of Physics and Electronic Engineering, Jiangsu Normal University, Xuzhou, Jiangsu, China

[2]School of Physics and Electronic Engineering, Changshu Institute of Technology, Changshu, Jiangsu, China

[3]Jiangsu Collaborative Innovation Center of Advanced Laser Technology and Emerging Industry, Jiangsu Normal University, Xuzhou, Jiangsu, China

[4]Qianjiang College, Hangzhou Normal University, Hangzhou, Zhejiang, China

[5]School of Chemistry and Materials Science, Jiangsu Normal University, Xuzhou, Jiangsu, China

Correspondence
Lulu Qu, 5 School of Chemistry and Materials Science, Jiangsu Normal University, Xuzhou, Jiangsu 221116, China.
Email: luluqu@jsnu.edu.cn

Caiqin Han, Jiangsu Collaborative Innovation Center of Advanced Laser Technology and Emerging Industry, Jiangsu Normal University, Xuzhou, Jiangsu 221116, China.
Email: hancq@jsnu.edu.cn

Funding information
Natural Science Foundation of Jiangsu Province, Grant/Award Numbers: BK20150227 and BK20151164; National Natural Science Foundation of China, Grant/Award Numbers: 21505057, 61575087 and 61771227

Abstract

A new method based on joint sparse representation is developed to recover the peak information from high-noise Raman signal. This method used the sparsity of Raman spectrum to recover the signals and preserve its useful peak information. The peak information is then reconstructed by using an orthogonal matching pursuit algorithm. The joint sparse representation method is found to be an effective approach to analyze the Raman spectrum, especially Raman spectrum that have high noise, thus improving the detection limit of Raman spectroscopy. Experimental results demonstrate that this approach is better than other approaches in case of low signal-to-noise ratios.

KEYWORDS

denoise algorithm, orthogonal matching pursuit, Raman spectroscopy, sparse representation

1 | INTRODUCTION

Raman spectroscopy is a powerful spectroscopic technique that is capable of qualitative or quantitative characterization of a wide range of substances such as inorganic materials, chemicals, and biological samples.[1–3] However, noise is a severe problem in Raman spectral analysis, which often obscures the characteristic

Raman bands.[4] One main noise source is the unspecific absorption of radiation by colored or black samples. The other is aroused by the charge-coupled device of Raman spectrometer, which causes at least three kinds of noises: the shot noise, the dark current noise, and the readout noise.[5] If these noises are not reduced, they will affect the quality of the calibration model and the accuracy of the Raman analysis. Generally, the best way to reduce noise is to use optimal experimental conditions and long time averaging of the signal. However, for some unstable materials and chemical reactions, short scanning time must be adopted to avoid damaging samples and observe a fast dynamic process, which will result in high background noise and low signal-to-noise ratio (SNR). Thus, it is urgent to develop new methods for the recovery of useful signals from the original spectra.

Many noise reduction methods have been exploited to analyze the Raman signals, such as finite impulse response (FIR) filtration,[6] Savitzky–Golay (S–G) filtration,[7,8] wavelet transform,[9,10] and empirical mode decomposition.[11] Among them, the FIR filtration is a linear filtration technique that can be designed to filter N numbers of its impulse responses with the specified filter length N. FIR filters are fully stable and easily implanted because there is a direct relationship between the frequency and the filter constants. The disadvantage of FIR is that it requires a lot of computation power. S–G filtration is a weighted mean method that exploits the different statistic characteristics of the signal and the noise. The various widths of the moving window affect the result significantly, but there is no definite and effective selection principle. Wavelet transform is based on the translations and dilations of wavelet basis functions to obtain features in time and frequency domain, whereas the choices of wavelet basis functions, the scale, and the threshold have a great impact on the result of denoising. Empirical mode decomposition decomposes the signal into different intrinsic mode functions adaptively according to the various time scales, and the high-frequency intrinsic mode functions should be removed. Moreover, the useful pure Raman signals can be easily obtained by the algorithms above when the noise level is not high.

In this paper, we propose a spectral processing method using joint sparse representation recovery by the orthogonal matching pursuit (OMP) algorithm.[12–14] The method having a strong anti-noise capability can achieve Raman spectrum directly due to its reconstruction principle. Another advantage of the proposed algorithm is that the peak information can be obtained without further processing.

2 | THEORY AND METHOD

2.1 | Sparse representation

Sparse representation has been attracting more and more interest in the signal processing field in recent years.[15] It is widely used for denoising, direction-of-arrival estimation of off-grid targets, and compressed sensing. A typical sparse representation problem employs the following linear model[16,17]:

$$y = Ds, \tag{1}$$

in which $D \in \mathbb{R}^{M \times N} (M \leq N)$ is a given dictionary matrix, it is an overcomplete dictionary. $y \in \mathbb{R}^M$ is a signal vector, and $s \in \mathbb{R}^N$ is the representation coefficient vector, which is known to be sparse, that is, the number of nonzero terms in s is far less than N.

In the research of sparse representation, the construction of dictionaries and the study of recovery algorithms computing sparse signal representation are closely related to a given dictionary. The dictionaries should be designed to better fit the model in Equation (1). Two kinds of dictionaries can be chosen in the sparse representation: selecting one from a prespecified set of linear transforms or learned dictionary. In this paper, the constructed dictionary is based on the signal model, and some details will be described in Section 2.3.

Traditional sparse representation can be solved using the following optimization problem[18]:

$$\min_s \|s\|_0 \text{ subject to } y = Ds \text{ or } \|y - Ds\|_2 \leq \varepsilon, \tag{2}$$

where $\|\cdot\|_0$ is l_0 norm to count the nonzero entries of a vector and the parameter ε represents how much noise we wish to allow. However, the solution of Equation (2) is too complex; in fact, it proves a NP-hard (nondeterministic polynomial time) problem, requiring traverse of all the sparse vectors. There is no currently known algorithm that can increase very quickly as the size of the problem grows. Thus, greedy methods and approximate solution methods based on convex relaxations are proposed in applications. The basis pursuit and the OMP algorithms are the most commonly used algorithms to compute sparse representations.

2.2 | Signal model

Generally, an observed Raman spectrum y can be modeled as follows:

$$y = P + e = \sum_{k=1}^{k} p_k + e, \tag{3}$$

where P represents the mixed peaks of interest, e is baseline contribution and Gaussian noise, and p_k represents

the lineshape function of the kth peak. In general, Raman spectrum is mathematically represented as Gaussian lineshape, Lorentzian lineshape, and Voigt lineshape.[19,20] The Gaussian lineshape, the Lorentzian lineshape, and the Voigt lineshape are used for the approximation of p_k as follows:

$$G_k(f) = a_k \exp\left[-\left(\frac{f-f_k}{b_k}\right)^2\right]. \quad (4)$$

The Gaussian lineshape is expressed by the formula (4), where f is the wavelength of each data point, f_k is the peak position, a_k is the amplitude, and b_k is the peak width.

$$L_k(f) = a_k \frac{1}{\left\{1 + \left[\frac{2(f-f_k)}{b_k}\right]^2\right\}} \quad (5)$$

The Lorentzian lineshape is expressed by the formula (5), where f is the wavelength of each data point, f_k is the peak position, a_k is the amplitude, and b_k is the full width at half maximum.

The Voigt lineshape can represented as

$$V_k(f) = c \cdot G_k(f) + (1-c) \cdot L_k(f), \quad (6)$$

where $G_k(f)$ is Gaussian function, $L_k(f)$ is Lorentzian function and c is the coefficient describing the proportion of the respective functions. Therefore, the position and intensity of the Raman peaks can be easily represented by the parameters in the above formulas.

2.3 | Dictionary construction

With the signal model of Raman spectrum taken into consideration, the direct method to estimate each peak is nonlinear parameter estimation algorithms. In our method, we attempt to find sparse approximation in terms of the approximation quality and sparsity of the signal itself. Finally, the peaks of interest $p_k(k = 1, ..., K)$ in Equation (3) are estimated by finding their joint sparse representations in the dictionary. Through some orthogonal transforms, we take the signals into informational domain and match the most important information, which makes the representation of Raman spectrum better. According to central wavelength of peaks, the dictionary is divided into K blocks $\{D_1, ..., D_m, ..., D_K\}$, where K is the number of interested peaks in a Raman spectrum. Different blocks have different number of basis functions. In this paper, we assume every block has the same basis function. So we constructed the dictionary as $\{d_1, d_2, ..., d_i, ...d_M\}$, where $M = K \times N$. The Raman spectrum can be denoted as follows:

$$P = Ds = \sum_{i=1}^{M} d_i s_i, \quad (7)$$

where s represents the sparse matrix and s_i represents the column of matrix.

2.4 | Recovery algorithm

OMP is a classical greedy algorithm in sparse representation, which has received much attention due to its simplicity and competitive reconstruction performance.

The algorithm is described as follows[14,21,22]:

Step 1: Initialize the residual $r_0 = y$ and initialize the set of selected variables $X(c_0) = \emptyset$. Let the iteration counter $i = 1$.
Step 2: Find the variable X_{t_i} that satisfies the condition $\max_t \left|X_t' r_{i-1}\right|$. Then, add the variable X_{t_i} to the set of selected variables. Update.
Step 3: Let $P_i = X(c_i)(X(c_i)'X(c_i))^{-1}X(c_i)'$, which is the projection onto the linear space spanned by the elements of $X(c_i)$. Update $r_i = (I - P_i)y$.
Step 4: If the stopping condition is reached, stop the algorithm. Otherwise, set $i = i + 1$ and return to Step 2.

The OMP is a stepwise forward selection algorithm and is easy to implement. A key component of OMP is the stopping rule that depends on the noise structure. In this paper, we shall consider the noise structures to decide the stopping rule.

3 | EXPERIMENT AND DISCUSSION

In this section, we test the proposed recovery method using both simulated and real Raman spectroscopy. To investigate the performance of the proposed method, we compared it with two other methods: wavelet transform and S–G filter. All computations and programmed algorithms were performed using Matlab software, which runs under the Microsoft Windows 7 Professional operating system. The detailed information about the method may be found in the Supporting Information.

3.1 | Simulation

On the basis of the spectral signal model, spectra were mathematically resolved into individual bands. Bands could be always represented as sums of distribution functions like the Gaussian function, the Lorentzian function, and the Voigt function. In this paper, a simulated spectrum containing three Gaussian peaks of different widths was used to evaluate the performance of the proposed method: peak position = [654, 1,002, 1,455 cm^{-1}], peak

amplitude = [500, 1,000, 1,500], and the peak half-width = [5, 8, 10]. The results of the three functions were shown in Figure 1. Figure 1a–c respectively shows the Gaussian function, the Lorentzian function, and the Voigt function as well as their own recovery signals. Compared with the original signals, there is no change in intensity and Raman shift, illustrating that the denoised process did not change the characteristics of Raman spectrum. Besides, the Raman signal obtained using our proposed method exhibited higher SNR, narrower half peak width, and smoother baseline compared with that of other methods (Figure 1d). This method can process Gaussian function, Lorentzian function, and Voigt function and recover the Raman signals successfully.

Moreover, Raman bands can be of different shapes except the symmetric bands. For this reason, we investigated the other two typical situations—asymmetric[23] and shoulder bands.[24] The result of asymmetric bands was shown in Figure 2a. The recovered signal can represent the peak position of asymmetric peak, but the band shape was affected. Similarly, the recovered signal of shoulder bands, which was shown in Figure 2b, represents the two peak positions, but the shape of shoulder was distorted.

In the present approach, the band shape will be affected because dictionaries are hard to construct for the recovery of half peak width. Hence, some analyses such as grain size, temperature variation, and crystallinity of crystals[25–27] will be not obtained due to the distortion of band shapes. This is also the boundedness of our method—the method is suitable for recovering positions and intensities of bands but unsuitable for recovering shapes of bands.

3.2 | Experiment

To further confirm whether the proposed method is effective for denoising the Raman signal, it is applied to processing the real spectra. The spectral measurements were performed on ProRaman-L analyzer from Enwave Optronics (Nd: frequency stabilized, narrow linewidth diode Laser [excitation line 785 nm], and two-dimensional charge-coupled devices array cooled with thermoelectric cooler). Figure 3a shows the surface-enhanced Raman scattering (SERS)[28] spectrum of 4-chloroaniline with the accumulating time of 0.2 s. We cannot observe the obvious peaks of 4-chloroaniline. The proposed algorithm is applied to the real Raman signal. According to literature, the peaks of the 4-chloroaniline were located near 637 and 1,602 cm^{-1}.[29] We focused on these two peaks in this study. The reconstructed SERS spectrum is smooth with the peak positions at 643 and 1,595 cm^{-1}, and their intensities were similar to those of the real Raman signals. Figure 3b compared the denoised SERS spectra of 4-chloroaniline processed by wavelet denoising,

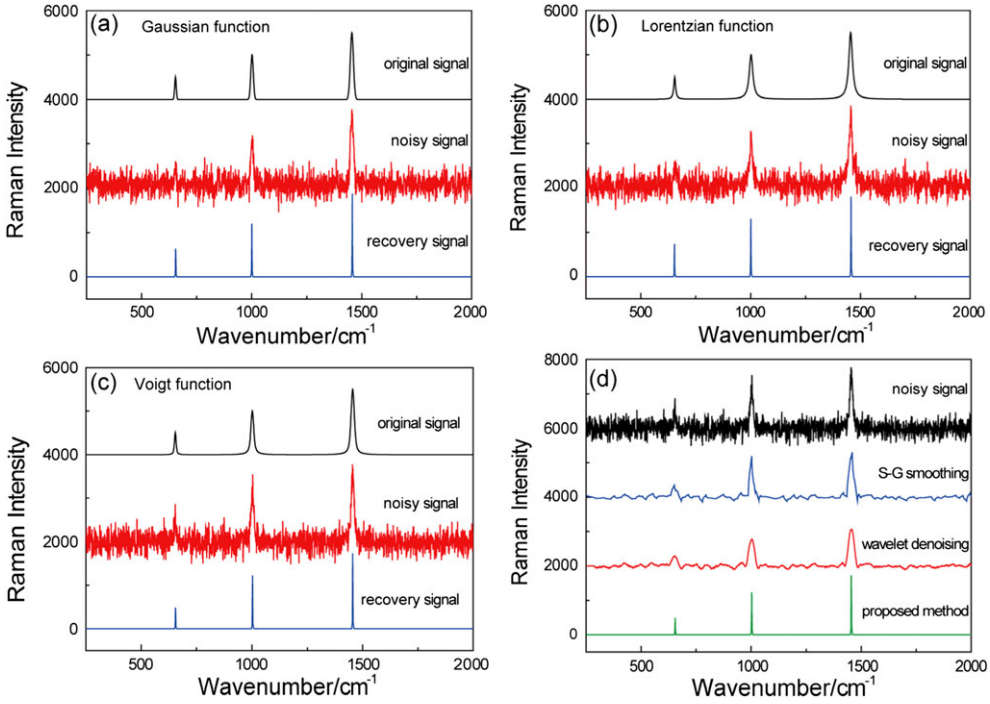

FIGURE 1 Simulation example by the proposed method: (a) Gaussian function signal; (b) Lorentzian function signal; (c) Voigt function signal; and (d) denoised signals of the Voigt function obtained by wavelet denoising, Savitzky–Golay (S–G) smoothing, and the proposed method [Colour figure can be viewed at wileyonlinelibrary.com]

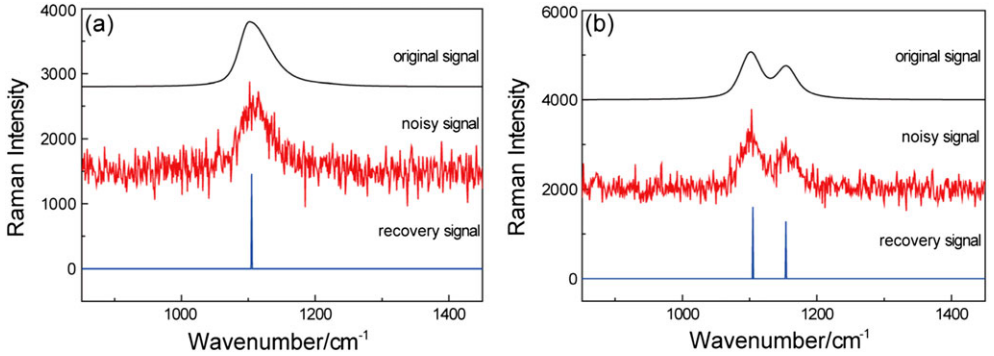

FIGURE 2 Two typical situations processed by the proposed method: (a) asymmetric signal and (b) shoulder bands signal [Colour figure can be viewed at wileyonlinelibrary.com]

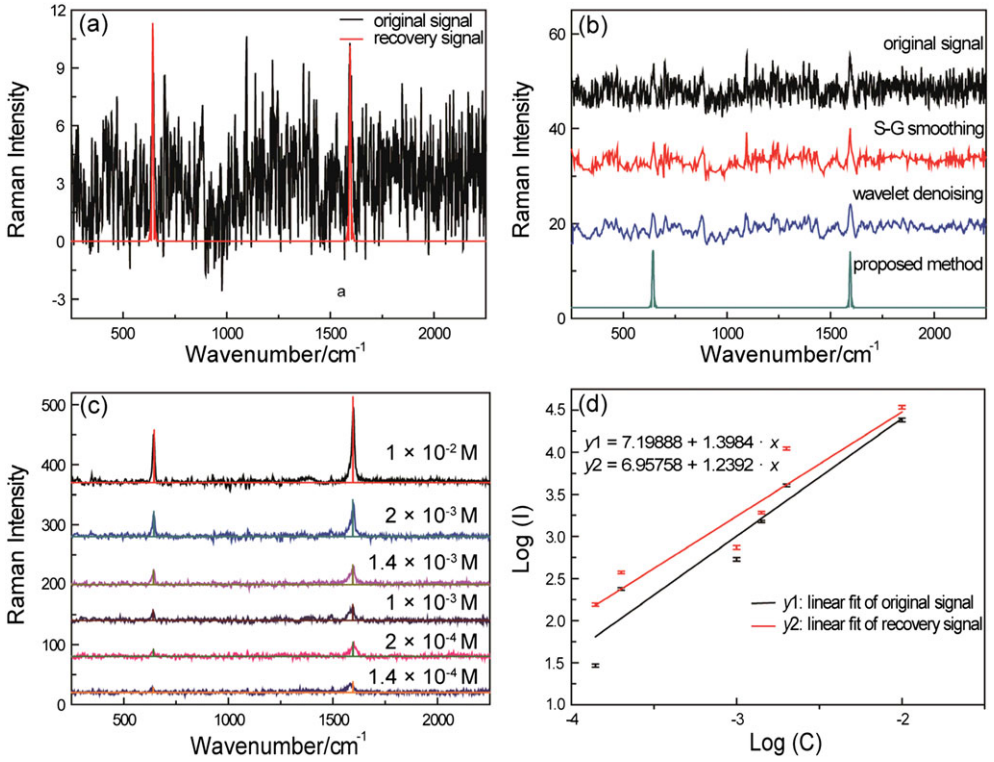

FIGURE 3 The experimental signal denoised by different methods: (a) experimental signal and denoised signal by proposed method; (b) denoised signals respectively by wavelet denoising, Savitzky–Golay (S–G) smoothing, and proposed method; (c) the original signals and recovery signals of different concentrations; (d) the linear relation between Raman peak intensity and concentrations of 4-chloroaniline at 643 cm^{-1} (logarithmic concentration and intensity) [Colour figure can be viewed at wileyonlinelibrary.com]

S–G smoothing, and proposed method. It is obvious that proposed method can reveal the characteristic peaks of analyte. Furthermore, we measured the Raman spectra of seven concentrations of 4-chloroaniline ($C = 1 \times 10^{-2}$, 2×10^{-3}, 1.4×10^{-3}, 1×10^{-3}, $2 \times 10^{-4}$and 1.4×10^{-4} M) in Figure 3c. The original signals can be fitted linearly by the function $y = 7.19888 + 1.3984 \cdot x$, the fitting yields the detection limit at 7.1×10^{-6} M. The processed signals' linear fit function is $y = 6.95758 + 1.2392 \cdot x$, and the detection limit is 2.4×10^{-6} M in Figure 3d. The detection limit is improved three times after the SERS spectra were processed using our proposed method, suggesting that the proposed method can improve the SNR and the detection limit of Raman signals.

4 | CONCLUSION

In this work, we have presented a novel and efficient recovery algorithm for Raman spectrum collected in short scanning time. This approach is suitable for reducing the

noise in Raman signals, and its efficiency is better than other methods in some aspects. Our method can recover the specific main peaks of a Raman spectrum, which is important to evaluate the Raman spectrum and detect the analytes. This makes the method well suited for the search of unknown signals buried in the random Gaussian noise. The method can be expanded to the quantitative analysis and improve the detection limit. The algorithm is also able to improve the signals' SNR of fast dynamic processes and unstable substance.

ACKNOWLEDGMENTS

This research is funded by the National Natural Science Foundation of China (Grant 61575087, 21505057, and 61771227) and the Natural Science Foundation of Jiangsu Province (Grant BK20151164 and BK20150227). The authors would like to thank a Project funded by the Priority Academic Program Development of Jiangsu Higher Education Institutions (PAPD).

REFERENCES

[1] T. G. Spiro, *J Raman Spectrosc* **1987**, *28*, 111.

[2] C. Han, Y. Yao, W. Wang, L. Qu, L. Bradley, S. Sun, Y. Zhao, *Sensors Actuators B Chem* **2017**, *251*.

[3] M. Yilmaz, E. Babur, M. Ozdemir, R. L. Gieseking, Y. Dede, U. Tamer, G. C. Schatz, A. Facchetti, H. Usta, G. Demirel, *Nat Mater* **2017**, *16*, 918.

[4] R. L. Mccreery, *Signal-to-Noise in Raman Spectroscopy*, John Wiley & Sons, Inc. **2005**.

[5] G. C. Holst. CCD arrays cameras and displays **1998**.

[6] Y. C. Lim, S. R. Parker, *IEEE Trans Acoust Speech Signal Process* **1983**, *31*, 583.

[7] Martin, c x, lupek, Mat P, b x, jka, Volka K, *J Raman Spectrosc* **2010**, *38*, 1174.

[8] K. M. T. Nahiyan, *Amin AA* **2017**, *8*, 32.

[9] P. M. Ramos, I. Ruisánchez, *J Raman Spectrosc* **2010**, *36*, 848.

[10] S. Khatun, R. Mahajan, B. I. Morshed, *IEEE J Transl Eng Health Med* **2016**, *4*, 1.

[11] A. Zahra, N. Kanwal, N. ur Rehman, S. Ehsan, K. D. McDonald-Maier, *Comput Biol Med* **2017**, *88*, 132.

[12] Z. Tan, P. Yang, A. Nehorai, *IEEE Trans Signal Process* **2014**, *62*, 4997.

[13] Y. C. Eldar, P. Kuppinger, H. Bolcskei, *IEEE Trans Signal Process* **2010**, *58*, 3042.

[14] J. A. Tropp, A. C. Gilbert, *IEEE Trans Inf Theory* **2007**, *53*, 4655.

[15] X. Fan, X. Wang, X. Wang, Y. Xu, J. Que, H. He, X. Wang, M. Tang, *J Instrum* **2016**, *11*, P02002.

[16] D. L. Donoho, *IEEE Trans Inf Theory* **2012**, *52*, 1289.

[17] M. Elad, *Sparse and Redundant Representations*, Springer New York **2010**.

[18] M. Protter, M. Elad, *IEEE Trans Image Process* **2009**, *18*, 27.

[19] T. Sundius, *J Raman Spectrosc* **1973**, *1*, 471.

[20] F. Herbert, *J Quant Spectrosc Radiat Transfer* **1974**, *14*, 943.

[21] T. T. Cai, L. Wang, *IEEE Trans Inf Theory* **2011**, *57*, 4680.

[22] C. Liu, Y. Fang, J. Liu, *IEEE Trans Signal Process* **2017**, *65*, 4511.

[23] V. I. Korepanov, D. M. Sedlovets, *Analyst* **2018**, *143*, 2674.

[24] V. Mochalin, S. Osswald, Y. Gogotsi, *Chem Mater* **2008**, *21*, 273.

[25] Z. Sun, J. Shi, B. Tay, S. Lau, *Diamond Relat Mater* **1979**, *2000*, 9.

[26] R. Cuscó, E. Alarcón-Lladó, J. Ibáñez, L. Artús, J. Jiménez, B. Wang, M. J. Callahan, *Phys Rev B* **2007**, *75*, 165202.

[27] C. Smit, R. Van Swaaij, H. Donker, A. Petit, W. Kessels, M. Van de Sanden, *J Appl Phys* **2003**, *94*, 3582.

[28] D. Graham, M. Moskovits, Z.-Q. Tian, *Chem Soc Rev* **2017**, *46*, 3864.

[29] E. Steger, S. Garbe, J. Klosowski, *J Raman Spectrosc* **2010**, *14*, 194.

SUPPORTING INFORMATION

Additional supporting information may be found online in the Supporting Information section at the end of the article.

How to cite this article: Fang Z, Tao Y, Wang W, et al. Joint sparse representation and denoising method for Raman spectrum. *J Raman Spectrosc*. 2018;1–6. https://doi.org/10.1002/jrs.5485